ELSEVIER

Thermochimica Acta 397 (2003) 67–73

thermochimica acta

www.elsevier.com/locate/tca

Low-temperature heat capacity and thermodynamic properties of crystalline [RE (Gly)$_3$(H$_2$O)$_2$]Cl$_3$·2H$_2$O (RE = Pr, Nd, Gly = Glycine)

Beiping Liu [a,b], Zhi-Cheng Tan [a,*], Jilin Lu [b], Xiao-Zheng Lan [a], Lixian Sun [a], Fen Xu [a], Ping Yu [a], Jun Xing [a]

[a] *Thermochemistry Laboratory, Dalian Institute of Chemical Physics, Chinese Academy of Sciences, Dalian 110623, China*
[b] *Department of Chemistry, Changde Normal College, Changde 415000, China*

Received 25 March 2002; accepted 3 May 2002

Abstract

Heat capacities of two solid complexes of rare-earth elements with glycine [RE(Gly)$_3$(H$_2$O)$_2$]Cl$_3$·2H$_2$O (RE = Pr, Nd, Gly = Glycine) have been measured with a high-precision automatic adiabatic calorimeter over the temperature range from 78 to 380 K. The melting point, molar enthalpy and entropy of fusion for the two complexes were determined on the basis of the heat capacity measurements. Thermal decompositions of the two complexes were studied by thermogravimetric (TG) techniques and a possible mechanism for the decompositions is suggested.

Keywords: [Pr(Gly)$_3$(H$_2$O)$_2$]Cl$_3$·2H$_2$O; [Nd(Gly)$_3$(H$_2$O)$_2$]Cl$_3$·2H$_2$O; Heat capacity; TG analysis; Rare-earth; Glycine

1. Introduction

Solid complexes of rare-earth elements with amino acids are important chemical substances, which are widely used in the wool dying industry as dying promoter and in agriculture as additive [1]. Since in 1975, Anghileri firstly reported that [La(Gly)$_3$(H$_2$O)]Cl$_3$·3H$_2$O has anti-tumor effect [2], rare-earth complexes with amino acids have been extensively studied because of their physiological and biochemical effects. Studying the interaction of rare-earth metal ions with amino acids can provide a large amount of information on biology effect and metabolism in living systems [3–7]. We must grasp many thermodynamic properties of these complexes before exploring this new research field. Heat capacity is one of the basic thermodynamic properties of substances and related to the structure and energetics of materials. However, until now, the low-temperature heat capacities and thermodynamic properties of rare-earth complexes with amino acids were scarcely reported in literature. Jin et al. [8] synthesized two single crystals of rare-earth chlorides (RE = Pr, Nd) with glycine, and measured their crystal structures.

In the present work, low-temperature heat capacities of two complexes [Pr(Gly)$_3$(H$_2$O)$_2$]Cl$_3$·2H$_2$O and [Nd(Gly)$_3$(H$_2$O)$_2$]Cl$_3$·2H$_2$O were measured over the temperature range from 78 to 380 K. At the same time, the molar enthalpies and entropies of fusion and the melting temperatures of the two complexes have

* Corresponding author. Tel.: +86-411-4379215; fax: +86-411-4691570.
E-mail address: tzc@dicp.ac.cn (Z.-C. Tan).

0040-6031/02/$ – see front matter
PII: S0040-6031(02)00293-9

been determined. In addition, possible mechanisms of thermal decompositions of the two complexes are proposed on the basis of thermogravimetric (TG) analysis.

2. Experimental

2.1. Sample synthesis and characterization

According to [8], rare-earth oxides (Pr_2O_3, Nd_2O_3, 99.9%), hydrochloric acid and glycine were used to prepare the experimental samples. First, the rare-earth oxides were dissolved in hydrochloric acid to get the aqueous solutions of the rare-earth chlordates, then the aqueous solutions were mixed with glycine at the mole ratio 1:3 at about pH = 3, which was regulated by adding a suitable amount of NaOH. The mixed solution was concentrated by evaporation, cooled and filtered. The filtrate placed into a desiccator with P_2O_5 until crystalline products isolate from the solutions. The crystals were filtered out and washed with anhydrous alcohol for three times. After this procedure, the colour changed to green and pink needle-like crystals. Finally, these crystals were desiccated in a dryer until their mass became constant.

The purity of the crystals was proved to be more than 99.90% by EDTA titrimetric analysis, good enough to meet the requirements of the present calorimetric study.

2.2. Adiabatic calorimeter

Heat-capacity measurements were carried out in a high-precision automatic adiabatic calorimeter described in detail elsewhere [9]. The principle of the calorimeter is based on the Nernst stepwise heating method. The calorimeter mainly consists of a sample cell, an adiabatic (or inner) shield, a guard (outer) shield, a platinum resistance thermometer, an electric heater, two sets of chromel–copel (Ni 55%, Cu 45%) thermocouples and a high vacuum can. The sample cell was made of gold-plated copper and had an inner volume of 6 cm^3. Four gold-plated copper vanes of 0.2 mm thickness were put into the cell to promote heat conduction from the cell to sample. The platinum resistance thermometer was inserted into a copper sheath which was soldered at the bottom of the sample cell. The heater wires were wound on the out wall of the cell. The lid of the cell with a copper capillary was sealed to the sample cell with cycleweld after the sample was loaded in it. The air in the cell was pumped out and a small amount of helium gas (0.1 MPa) was introduced into it to enhance the heat transfer in the cell. The capillary was pinched off and the resultant fracture was soldered with a little amount of solder to ensure the cell for sealing. The evacuated can was kept within ca. 10^{-3} Pa during the heat-capacity measurements so as to eliminate the heat loss due to gas convection. Liquid nitrogen was used as the cooling medium. One set of chromel–copper thermocouples were used to detect the temperature difference between the sample cell and the inner shield. Likewise, another set of thermocouples was installed between the inner and outer shields. The temperature difference between them was kept to be 0.5 mK during the whole experimental process. The sample cell was heated by the standard discrete heating method. The temperature of the cell was alternatively measured. The temperature increment for a heating period was 2–4 K, and temperature drift was maintained at about 10^{-3} K min^{-1} in equilibrium period. All the data were automatically picked up through a Data Acquisition/Switch Unit (Model: 34970A, Aglient, USA) and processed by a computer.

The mass of the $[Pr(Gly)_3(H_2O)_2]Cl_3{\cdot}2H_2O$ and $[Nd(Gly)_3(H_2O)_2]Cl_3{\cdot}2H_2O$ used for heat-capacity measurements was 1.3802 and 1.6322 g, which are equivalent to 0.002535 and 0.002980 mol, based on their corresponding molar mass of 544.467 and 547.76 g mol^{-1}, respectively.

To verify the reliability of the adiabatic calorimeter, the molar heat capacities for the reference standard material α-Al_2O_3 were measured. The mass of α-Al_2O_3 used for the measurement was 1.6382 g, which was equivalent to 0.01607 mol based on its molar mass $M(Al_2O_3) = 101.9613$ g mol^{-1}. The deviations of our experimental results from the recommended values of the National Bureau of Standards [10] were within ±0.2% in the temperature range of 80–400 K.

2.3. Thermal analysis

A thermogravimetric analyzer (Model TGA/SDTA 851 e, METTLER TOLEDO, Switzerland) was used for TG measurements of the solid complexes under high purity (99.999%) nitrogen atmosphere

with a flow rate of 60 ml min^{-1}. The masses of the samples used for TG analysis were 1.3180 and 1.7220 mg for $[Pr(Gly)_3(H_2O)_2]Cl_3{\cdot}2H_2O$ and $[Nd(Gly)_3(H_2O)_2]Cl_3{\cdot}2H_2O$, respectively. The heating rate was 10 K min^{-1}.

3. Results and discussion

3.1. Heat capacity

The low-temperature experimental molar heat capacities of the solid complexes are shown in Fig. 1 and listed in Tables 1 and 2, respectively. The molar heat capacities of the samples are fitted to the following polynomials in reduced temperature (X) by means of the least square fitting.

For the solid complex $[Pr(Gly)_3(H_2O)_2]Cl_3{\cdot}2H_2O$, over the temperature ranges from 80 to 353 K and from 364 to 377 K,

$$C_{p,m}\ (J\,K^{-1}\,mol^{-1}) = 372.2648 + 322.5773X - 162.2029X^2 - 435.236X^3 + 222.7372X^4 + 381.9981X^5 \quad (1)$$

where $X = (T(K)-229)/149$, T is the absolute temperature. The correlation coefficient of the fitting, $R^2 = 0.9928$.

For the solid complex $[Nd(Gly)_3(H_2O)_2]Cl_3{\cdot}2H_2O$, over the temperature ranges from 78 to 297 K,

$$C_{p,m}\ (J\,K^{-1}\,mol^{-1}) = 327.5839 + 181.2793X + 209.2867X^2 - 171.6420X^3 - 485.3327X^4 + 143.2519X^2 + 312.8039X^6 \quad (2)$$

where $X = (T(K)-187.5)/109.5$, the correlation coefficient, $R^2 = 0.9960$.

From Fig. 1, it can be seen that the heat capacities of the two complexes increase with increasing temperature in a smooth and continuous manner in the temperature range from 78 to 297 K for $[Nd(Gly)_3(H_2O)_2]Cl_3{\cdot}2H_2O$, from 78 to 350 K for $[Pr(Gly)_3(H_2O)_2]Cl_3{\cdot}2H_2O$, which indicate that the two complexes are stable in the above temperature ranges. The melting peaks were observed at 323.72 K for $[Nd(Gly)_3(H_2O)_2]Cl_3{\cdot}2H_2O$, at 359.35 K for $[Pr(Gly)_3(H_2O)_2]Cl_3{\cdot}2H_2O$, respectively.

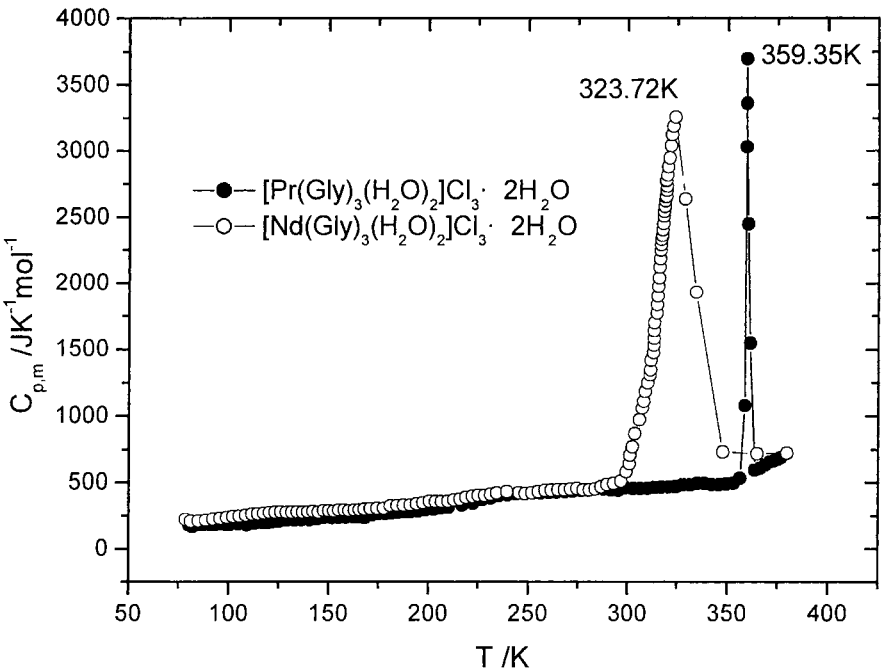

Fig. 1. Experimental heat-capacity of $[RE(Gly)_3(H_2O)_2]Cl_3{\cdot}2H_2O$ (RE = Pr, Nd) as a function of temperature.

Table 1
The experimental molar heat capacities of $[Pr(Gly)_3(H_2O)_2]Cl_3{\cdot}2H_2O$ (molar mass: $M = 544.47$)

T (K)	C_p ($J\,K^{-1}\,mol^{-1}$)	T (K)	C_p ($J\,K^{-1}\,mol^{-1}$)	T (K)	C_p ($J\,K^{-1}\,mol^{-1}$)
80.276	170.47	166.071	245.19	291.721	447.97
81.910	172.00	168.263	249.22	295.455	454.23
84.486	175.97	171.702	254.53	299.198	454.45
86.983	178.93	175.060	260.45	302.918	456.69
89.403	181.44	178.392	266.11	306.615	458.99
91.776	182.31	181.693	270.43	310.298	461.68
94.091	184.54	184.967	275.25	313.905	466.13
96.358	185.15	188.214	280.15	317.264	467.46
98.588	186.02	191.437	282.41	320.887	470.14
100.776	186.72	194.975	285.33	324.511	471.47
102.922	187.37	198.819	293.83	328.046	480.50
105.042	188.79	202.625	299.41	331.670	483.50
107.143	191.67	206.394	307.60	335.146	484.00
109.172	192.47	210.135	313.05	338.799	486.49
111.211	193.45	216.964	331.02	342.501	488.38
113.214	194.55	222.448	345.95	346.094	490.69
115.190	196.89	226.861	365.10	349.675	492.75
117.150	197.47	231.231	385.91	353.247	497.73
119.397	200.07	235.552	401.42	356.512	535.22
121.910	203.40	239.773	410.64	358.675	1081.15
125.169	207.36	244.016	416.64	359.347	3033.39
129.135	212.40	248.215	421.38	359.349	3697.93
133.017	216.99	252.369	422.33	359.470	3362.09
136.829	219.86	256.478	424.17	360.104	2449.63
140.585	221.39	260.548	425.03	361.419	1547.70
144.285	225.54	264.587	429.95	363.858	597.61
147.925	230.72	268.594	432.77	366.495	609.74
151.533	233.38	272.570	437.21	368.994	633.34
155.097	237.09	276.509	441.06	371.266	658.23
158.622	239.29	280.389	445.73	373.377	665.69
162.906	240.19	284.231	446.03	375.162	678.13
165.179	243.93	287.987	447.70	376.705	690.57

3.2. The melting point, molar enthalpy and molar entropy of fusion

The melting temperature of the samples was obtained from the $C_p(T)$ curves. The peak temperature of the heat-capacity curves (Fig. 1) of the samples was selected as the melting point T_m. The molar enthalpies ΔH_m, and molar entropies ΔS_m, of the melting transition can be calculated based on the following equations:

$$\Delta H_m = \frac{Q - n\int_{T_i}^{T_m} C_{p,1}\,dT - n\int_{T_m}^{T_f} C_{p,2}\,dT - n\int_{T_i}^{T_f} H_0\,dT}{n} \quad (3)$$

$$\Delta S_m = \frac{\Delta H_m}{T_m} \quad (4)$$

where T is the temperature a few degrees lower than the initial melting temperature, T_f is a temperature slightly higher than the final melting temperature, Q is the total energy introduced into the sample cell from T_i to T_f, H_0 is the heat capacity of the sample cell from T_i to T_f, C_{p1} the heat capacity of the sample in solid phase from T_i to T_m, C_{p2} the heat capacity of the sample in liquid phase from T_m to T_f, and n is molar amount of the sample. The melting point, molar enthalpy and molar entropy of fusion were determined to be 359.35 K, 6.60 and 18.37 $J\,K^{-1}\,mol^{-1}$ for $[Pr(Gly)_3(H_2O)_2]Cl_3{\cdot}2H_2O$,

Table 2
The experimental molar heat capacities of $[Nd(Gly)_3(H_2O)_2]Cl_3{\cdot}2H_2O$ (molar mass: $M = 547.76$)

T (K)	C_p ($J\,K^{-1}\,mol^{-1}$)	T (K)	C_p ($J\,K^{-1}\,mol^{-1}$)	T (K)	C_p ($J\,K^{-1}\,mol^{-1}$)
78.364	202.18	200.513	354.91	311.607	1346.59
81.131	208.90	203.694	357.91	311.696	1418.74
84.987	211.80	206.788	359.24	313.021	1474.85
88.676	218.20	209.881	364.91	313.110	1533.64
92.236	224.98	212.886	372.60	313.287	1583.07
95.698	231.28	215.979	377.95	313.375	1640.52
99.060	237.55	218.984	389.97	313.552	1699.31
102.332	243.24	222.078	399.32	314.789	1772.79
105.526	249.42	225.171	406.34	314.966	1836.92
108.652	255.08	228.353	410.00	315.143	1902.39
111.710	261.62	231.269	414.02	315.496	1974.54
114.716	266.88	234.274	423.37	315.850	2042.68
117.662	271.83	239.400	424.73	316.026	2121.50
120.567	276.57	245.410	425.97	316.292	2186.97
123.425	279.56	248.580	426.62	316.468	2251.10
126.246	280.00	251.907	430.66	316.645	2292.52
129.030	280.03	255.219	435.04	316.910	2333.94
131.775	280.18	258.509	441.66	317.175	2363.33
134.491	281.36	261.777	445.82	317.440	2406.08
137.178	281.79	265.021	450.68	317.706	2452.85
139.836	281.93	268.254	452.69	317.971	2510.30
142.473	283.73	271.453	453.10	318.148	2543.70
145.092	285.47	274.623	455.82	318.413	2581.11
147.661	288.10	277.774	457.30	318.589	2623.86
150.224	289.77	280.842	460.09	318.855	2654.59
152.787	290.10	283.881	464.81	319.120	2657.26
155.350	291.11	286.886	470.46	319.385	2701.35
157.913	293.11	289.858	486.74	319.562	2733.42
160.476	294.44	293.150	496.06	319.031	2773.50
163.039	295.78	296.848	513.99	319.120	2778.84
165.54	298.45	299.590	584.25	319.650	2820.26
167.988	301.79	301.090	641.15	320.004	2883.06
170.993	304.46	301.267	705.28	320.711	2949.86
174.440	308.47	302.504	770.75	321.506	3040.71
177.799	313.47	303.830	868.28	321.948	3123.55
181.157	319.18	306.128	973.83	322.655	3187.68
184.427	325.51	307.453	1060.67	323.716	3258.49
187.697	331.19	308.249	1111.44	328.753	2637.22
190.967	335.19	308.868	1186.26	334.410	1931.78
194.149	343.21	310.193	1251.73	348.020	732.47
197.331	349.89	311.431	1310.52	364.840	729.61
				379.772	724.94

to be 323.72 K, 57.91 and 178.90 $J\,K^{-1}\,mol^{-1}$ for $[Nd(Gly)_3(H_2O)_2]Cl_3{\cdot}2H_2O$, respectively.

3.3. TG results

The TG curve of $Pr(Gly)_3(H_2O)_2]Cl_3{\cdot}2H_2O$ is shown in Fig. 2. It can be seen clearly from the mass-loss curve that most of the activities occur in the temperature range of 272–579 °C. The solid complex was stable below 100 °C, and started decomposition at 114 °C. The total mass-loss (%) is 40.88%. We consider that the residue should be $PrCl_3$ because the mass loss (%) calculated theoretically is 41.37% if the final residual is $PrCl_3$.

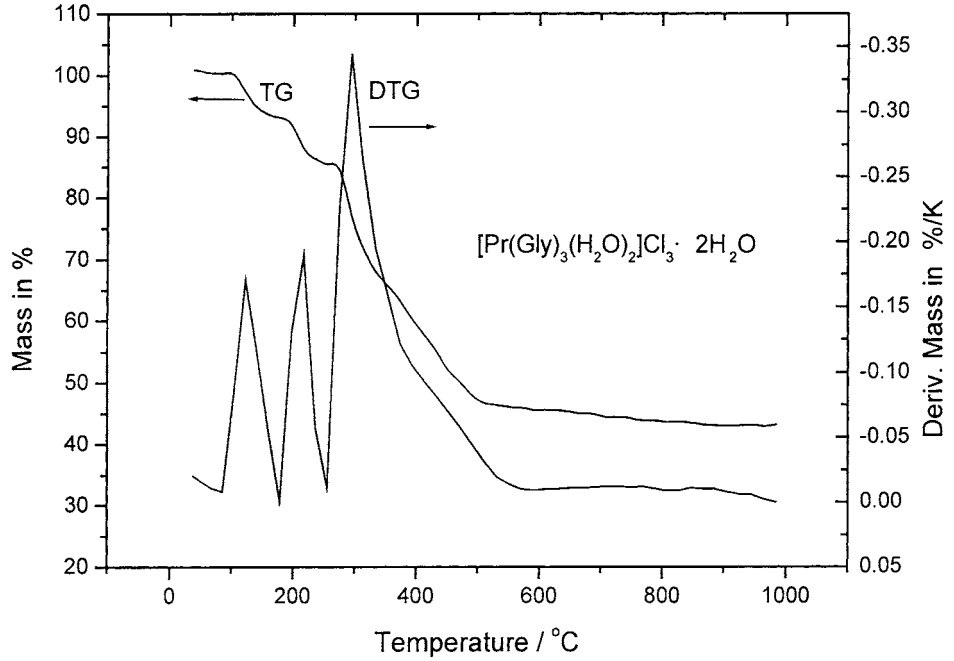

Fig. 2. TG/DTG curve of $[Pr(Gly)_3(H_2O)_2]Cl_3{\cdot}2H_2O$ under nitrogen atmosphere.

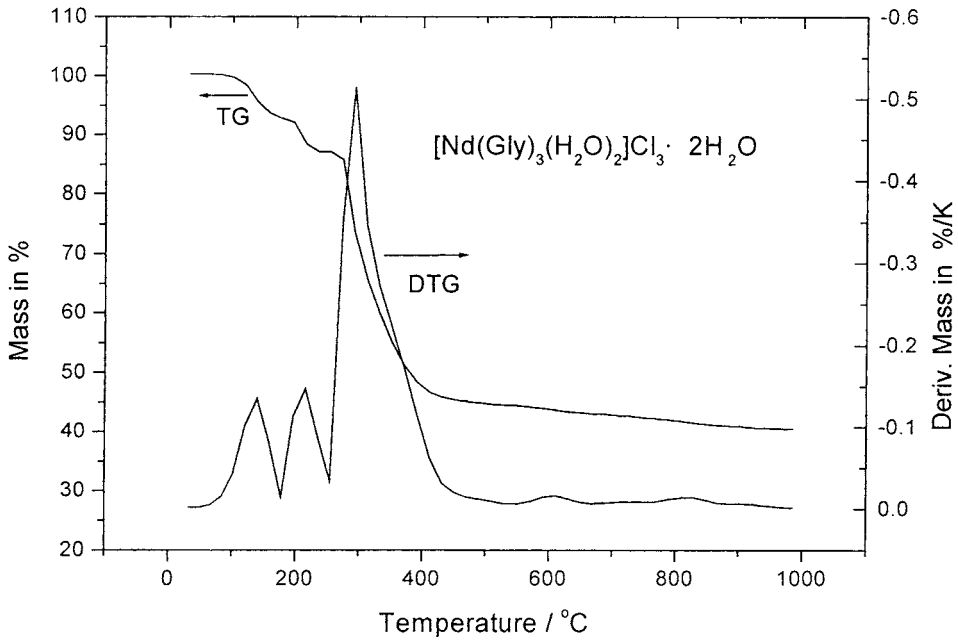

Fig. 3. TG/DTG curve of $[Nd(Gly)_3(H_2O)_2]Cl_3{\cdot}2H_2O$ under nitrogen atmosphere.

Fig. 3 shows that the structure of $[Nd(Gly)_3(H_2O)_2]Cl_3{\cdot}2H_2O$ is stable below 100 °C. It starts mass-loss at 105 °C. The experiment result of final mass-loss was 42.28%, which suggested that the residual product should be $NdCl_3$, because the theoretical mass-loss (%) of the decomposition is 41.11% when the final residual is $NdCl_3$. According to the mass-loss in each step, a possible mechanisms of the thermal decompositions may be as follows:

$$[Pr(Gly)_3(H_2O)_2]Cl_3 \cdot 2H_2O \xrightarrow[6.89\%(6.61\%)]{114-157\,^\circ C} [Pr(Gly)_3(H_2O)_2]Cl_3 \xrightarrow[6.22\%(6.61\%)]{178-255\,^\circ C} [Pr(Gly)_3]Cl_3 \xrightarrow[40.88\%(41.71\%)]{272-579\,^\circ C} PrCl_3$$

and

$$[Nd(Gly)_3(H_2O)_2]Cl_3 \cdot 2H_2O \xrightarrow[6.33\%(6.57\%)]{105-167\,^\circ C} [Nd(Gly)_3(H_2O)_2]Cl_3 \xrightarrow[6.87\%(6.57\%)]{180-255\,^\circ C} [Nd(Gly)_3]Cl_3 \xrightarrow[42.28\%(41.11\%)]{260-531\,^\circ C} NdCl_3$$

Acknowledgements

The authors gratefully acknowledge the National Nature Science Foundation of China for financial support to this work under NSFC Grant no. 20073047.

References

[1] J.Y. Fang, T.Z. Jin, G.G. Xu, J. Xie, Chin. Acta Rare Earth Met. 3 (1984) 2.
[2] L.J. Anghileri, Arzneim-Forsch 25 (1975) 793.
[3] J.X. Chen, Z.Z. Guo, X.Q. Ran, J. Chem. Chin. Univ. 11 (1990) 555.
[4] S.L. Gao, X.W. Yang, D.H. Ren, Thermochim. Acta 287 (1996) 177.
[5] S.L. Gao, H.F. Xue, W.L. Zhang, Acta Chim. Sinica 52 (1994) 693.
[6] X.W. Jiang, Y.M. Chen, S.L. Gao, Chin. Sci. Bull. 38 (1993) 129.
[7] S.L. Gao, Y.L. Lu, Z.P. Yang, J. Rare Earth 11 (1990) 3.
[8] T.Z. Jin, C.Q. Yang, Q.C. Yang, J.U. Wu, G.X. Xu, J. Chem. Chin. Univ. 10 (1989) 118.
[9] Z.C. Tan, G.Y. Sun, Y. Sun, A.X. Yin, W.B. Wang, J.C. Ye, L.X. Zhou, J. Therm. Anal. 45 (1995) 59.
[10] D.A. Ditmars, S. Ishihara, S.S. Chang, G. Bernstein, B.D. West, J. Res. Natl. Bur. Stand. 87 (1982) 159.